

## Synthesis and crystal structure of new $\text{PbBaFe}_{2-x}\text{Mn}_x\text{O}_5$ perovskite-type compounds

P. Tzvetkov<sup>1\*</sup>, D. Kovacheva<sup>1</sup>, D. Nihtianova<sup>1,2</sup>, N. Velichkova<sup>1</sup>, T. Ruskov<sup>3</sup>

<sup>1</sup> Institute of General and Inorganic Chemistry, Bulgarian Academy of Sciences  
1113 Sofia "Acad. Georgi Bonchev" str. bld.11

<sup>2</sup> Institute of Mineralogy and Crystallography, Bulgarian Academy of Sciences  
1113 Sofia "Acad. Georgi Bonchev" str. bld.107

<sup>3</sup> Institute for Nuclear Research and Nuclear Energy, Bulgarian Academy of Sciences  
1784 Sofia "Tzarigradsko chaussee" 72 Blvd.

Received March 22, 2012; Revised April 27, 2012

New perovskite-based compounds with general formula  $\text{PbBaFe}_{2-x}\text{Mn}_x\text{O}_5$  ( $0 \leq x \leq 1.5$ ) were synthesized by solid-state reaction under argon atmosphere. The compounds were characterized by X-ray powder diffraction, TEM (SAED) and <sup>57</sup>Fe Mössbauer spectroscopy. The crystal structure of  $\text{PbBaFeMnO}_5$  and  $\text{PbBaFe}_{0.5}\text{Mn}_{1.5}\text{O}_5$  members of the series is determined by Rietveld refinement method. The basic crystallographic sections in orientations [100] and [010] are obtained by SAED method. The Rietveld refinement results are in good agreement with the SAED data. The compounds crystallize in the orthorhombic space group *Pnma* with unit cell parameters  $a \approx \sqrt{2}a_p$ ,  $b \approx a_p$ , and  $c \approx 4\sqrt{2}a_p$  ( $a_p$  – the parameter of the perovskite subcell). The crystal structure of the studied phases consists of perovskite blocks separated by  $\frac{1}{2}[110]_p(\bar{1}01)_p$  ( $p$  – the perovskite subcell) crystallographic shear planes. Inside the blocks the octahedral B–position is occupied by  $\text{Fe}^{3+}$  and  $\text{Mn}^{3+}$  ions and the twelve coordinated A–position is fully occupied by  $\text{Ba}^{2+}$  ions. The perovskite blocks are connected to each other by double chains of edge-sharing (Fe, Mn) $\text{O}_5$  distorted tetragonal pyramids running along the  $b$ –axis. The double chains delimit six-sided tunnels fully occupied by  $\text{Pb}^{2+}$  cations. The pyramidal chains adopt two mirror-related configurations ("left" L and "right" R) and layers consisting of chains of the same configuration alternate along the  $c$ –axis in –L–R–L–R– sequence. The Mössbauer spectroscopy reveals a transition from magnetic ordering to paramagnetic state in  $\text{PbBaFe}_{1.5}\text{Mn}_{0.5}\text{O}_5$  at room temperature with the substitution of  $\text{Fe}^{3+}$  by  $\text{Mn}^{3+}$  cations. The measurements at 77 K show that the  $\text{Mn}^{3+}$  cations replace the  $\text{Fe}^{3+}$  cations for the octahedral (1) and the pyramidal (2) sites in equal proportions.

**Key words:** perovskites, crystallographic shear planes, cation substitutions.

### INTRODUCTION

Perovskite-type compounds with general formula  $\text{ABO}_3$  are extensively studied for many years due to their various electric and magnetic properties: dielectrics, high temperature superconductors, ion conductors, colossal magneto-resistant materials, optical materials, etc. The perovskite structure consists of cubic close packing of oxygen atoms and A-cations, with  $\frac{1}{4}$  of the octahedral interstices occupied by B-cations. Many structures can be derived from that of perovskite by various ways: by mixed occupancy and cation ordering in A and B positions; vacancy ordering in the cation and anion sublattices;

intergrowth of perovskite and other structure type blocks ( $\text{NaCl}$ ,  $\text{CaF}_2$  and other structure types) and the formation of hexagonal perovskite polytypes. The oxygen vacancies ordering in the perovskite structure gives rise to many compounds with different structures ( $\text{Ca}_2\text{Mn}_2\text{O}_5$ ,  $\text{La}_2\text{Ni}_2\text{O}_5$ ,  $\text{Ca}_2\text{Fe}_2\text{O}_5$ ) [1, 2]. Recently, new class of oxygen deficient perovskite-type compounds incorporating periodically ordered translational interfaces was synthesized. The first published member of the class is  $\text{Pb}_{1.33}\text{Sr}_{0.67}\text{Fe}_2\text{O}_5$  (*Pnma*,  $a = 5.687 \text{ \AA}$ ,  $b = 3.920 \text{ \AA}$ ,  $c = 21.075 \text{ \AA}$ ) [3] with relations to the perovskite subcell ( $a_p$ ):  $a \approx \sqrt{2}a_p$ ,  $b \approx a_p$ ,  $c \approx 4\sqrt{2}a_p$ . The structure can be described as an anion deficient perovskite in which half of the  $\text{B}^{3+}$  cations are located in octahedral coordination as in the prototype perovskite structure and the other half are five-coordinated in distorted tetragonal pyramids. The pyramids

\* To whom all correspondence should be sent:  
E-mail: p-tzvetkov@gmx.net

share common edges and form double chains and channels between them along the b-axis, alternating with perovskite blocks along the c-axis. Inside the channels the Pb<sup>2+</sup> cations are coordinated by six oxygen atoms and one 6s<sup>2</sup> electron lone pair of the lead atom. The A<sup>2+</sup> cation position is situated within the perovskite block and has mixed occupancy by Pb<sup>2+</sup> and Sr<sup>2+</sup> ions. The introduction of periodically ordered translational interfaces into the perovskite structure was based on the basis of detailed transmission electron microscopy investigations of Pb and Fe-containing compounds [4, 5, 6]. The translational interfaces were found to have similar crystallographic properties as the crystallographic shear planes (CS planes) in ReO<sub>3</sub> structure type. The structure of Pb<sub>1.33</sub>Sr<sub>0.67</sub>Fe<sub>2</sub>O<sub>5</sub> incorporates alternating CS planes and perovskite blocks along the c – axis. The shear planes remove a layer of oxygen atoms and displace the perovskite blocks with respect to each other by 1/2[110]<sub>p</sub> vector. Derivative compounds of Pb<sub>1.33</sub>Sr<sub>0.67</sub>Fe<sub>2</sub>O<sub>5</sub> with different chemical composition and thickness of the perovskite block are part of the homologous series A<sub>n</sub>B<sub>n</sub>O<sub>3n-2</sub> (n = 4, 5, 6) (A = Pb, Ba, Bi; B = Fe, Co, Mn, Ti, Sn) [7]. Chemical compositions Pb<sub>1.33</sub>Sr<sub>0.67</sub>Fe<sub>2</sub>O<sub>5</sub> [3], Pb<sub>1.33</sub>Sr<sub>0.67-x</sub>Ba<sub>x</sub>Fe<sub>2</sub>O<sub>5</sub> (0 ≤ x ≤ 0.67) [8], Pb<sub>2-x</sub>Ba<sub>x</sub>Fe<sub>2</sub>O<sub>5</sub> (0.6 ≤ x ≤ 1.0) [9], Pb<sub>2</sub>Mn<sub>2</sub>O<sub>5</sub> [10] and PbBaFe<sub>2-x</sub>Co<sub>x</sub>O<sub>5</sub> (0 ≤ x ≤ 1) [11] represents the n = 4 member of the homologous series. Partial replacement of B<sup>3+</sup> by other cation with formal charge 4+ can enlarge the thickness of the perovskite block as compared to the prototype Pb<sub>1.33</sub>Sr<sub>0.67</sub>Fe<sub>2</sub>O<sub>5</sub> structure. The members of the series Pb<sub>2.9</sub>Ba<sub>2.1</sub>Fe<sub>4</sub>TiO<sub>13</sub> and Pb<sub>2.85</sub>Ba<sub>2.15</sub>Fe<sub>4</sub>SnO<sub>13</sub> (n = 5) [12, 13] and Pb<sub>3.8</sub>Bi<sub>0.2</sub>Ba<sub>2</sub>Fe<sub>4.2</sub>Ti<sub>1.8</sub>O<sub>16</sub> (n = 6) [12] represent 1.5 (n = 5) and 2 (n = 6) times the thickness of perovskite block.

In this work we report on the synthesis and crystal structure of PbBaFe<sub>2-x</sub>Mn<sub>x</sub>O<sub>5</sub> (0 ≤ x ≤ 1.5) solid solution, a new member of the homologous series A<sub>n</sub>B<sub>n</sub>O<sub>3n-2</sub> (n = 4).

## EXPERIMENTAL

Polycrystalline samples with chemical composition PbBaFe<sub>2-x</sub>Mn<sub>x</sub>O<sub>5</sub> (0 ≤ x ≤ 1.5, Δx=0.25) were prepared by high temperature solid state reaction. Analytical grade PbO, BaCO<sub>3</sub>, Fe<sub>2</sub>O<sub>3</sub> and MnO were used as starting compounds. Stoichiometric mixtures of the reagents were homogenized in agate mortar with acetone and pressed into pellets. The pellets were heated at 800 °C for 24 hours in argon flow with intermediate regrinding every 6 hours. After each regrinding the samples were annealed at 400 °C for 1 hour in air.

Powder X-ray diffraction (XRD) patterns were collected at room temperature on Bruker D8 Advance

diffractometer using CuKα radiation and LynxEye PSD detector within the range 13–130° 2θ, step 0.02° 2θ and 6 sec/strip (total of 1050 sec/step) counting time. To improve the statistics, sample rotating speed of 30 rpm was used. The crystal structure parameters were refined using TOPAS 4.2 program [14].

The TEM (SAED) investigations were performed by transmission electron microscope JEOL 2100 at 200 kV accelerating voltage. The specimens were grinded and dispersed in ethanol by ultrasonic treatment for 6 min. The suspensions were dripped on standard holey carbon/Cu grids.

Mössbauer measurements were performed using a constant acceleration spectrometer. A source of <sup>57</sup>Co(Rh) with activity of 50 mCi was used. The PbBaFe<sub>1.5</sub>Mn<sub>0.5</sub>O<sub>5</sub> spectra were taken in the transmission mode at room temperature and at 77 K. The sample with a thickness of 50 mg cm<sup>-2</sup> was mounted in a cryostat of He exchange cooling gas. The Mössbauer spectra were fitted using an integral Lorentzian line shape approximation or thin sample approximation [15, 16]. The isomer shifts are referred to the centroid of α-iron foil reference spectrum at room temperature. The geometric effect is taken into account as well.

## RESULTS AND DISCUSSION

Single phase samples of PbBaFe<sub>2-x</sub>Mn<sub>x</sub>O<sub>5</sub> were obtained for x = 0, 0.25, 0.5, 0.75, 1.0, 1.25 and 1.5. The powder XRD patterns of all samples were indexed in orthorhombic symmetry, space group *Pnma* and unit-cell parameters a ≈ √2a<sub>p</sub>, b ≈ a<sub>p</sub>, c ≈ 4√2a<sub>p</sub>. To prevent the oxidation of Mn<sup>3+</sup> to Mn<sup>4+</sup> and the formation of BaMnO<sub>3</sub> as additional phase, all manganese containing samples were synthesised in argon flow. Since lead oxide starts to evaporate at temperatures above 800 °C to compensate possible losses an excess of 3% wt. was added to the stoichiometric mixture. The samples with higher Mn content (x > 1.5) are beyond the homogeneity range and contain PbO (Massicot) and BaFeO<sub>2.25</sub> as impurity phases. Samples PbBaFeMnO<sub>5</sub> and PbBaFe<sub>0.5</sub>Mn<sub>1.5</sub>O<sub>5</sub> were chosen for detailed structural investigation. The starting unit cell parameters and zero shift value were determined during the preliminary characterization using the whole powder pattern matching procedure (Pawley fit) (Table 1). The XRD phase analysis of PbBaFeMnO<sub>5</sub> and PbBaFe<sub>0.5</sub>Mn<sub>1.5</sub>O<sub>5</sub> revealed a single phase for the first sample and small impurities of PbO – Massicot in the last one. The determined amount of PbO from the Rietveld refinement is 2.73% wt. The Pawley fit of XRD patterns during the preliminary characterization of both samples revealed considerable

**Table 1.** Unit-cell parameters for PbBaFe<sub>2-x</sub>Mn<sub>x</sub>O<sub>5</sub> (0 ≤ x ≤ 1.5)

<i>x</i>	<i>a</i> (Å)	<i>b</i> (Å)	<i>c</i> (Å)
0.00	5.7656(2)	3.9920(1)	21.1433(6)
0.25	5.7661(4)	3.9733(3)	21.176(2)
0.50	5.7806(4)	3.9510(3)	21.281(2)
0.75	5.7839(6)	3.9382(4)	21.311(2)
1.00	5.7994(3)	3.9095(3)	21.407(1)
1.25	5.8123(3)	3.8962(2)	21.4752(8)
1.50	5.8182(2)	3.8816(1)	21.5115(5)

anisotropic peak shape broadening. The structure refinement without introducing a model for describing the anisotropic peak shapes leads to  $R_B = 2.28$  and  $R_B = 2.21$  respectively. Satisfactory results were achieved by using 8<sup>th</sup> order spherical harmonics [17]. The reliability factors show considerable improvement of  $R_B = 1.59$  and 1.76 for PbBaFeMnO<sub>5</sub> and PbBaFe<sub>0.5</sub>Mn<sub>1.5</sub>O<sub>5</sub>, respectively. The observed anisotropic line broadening is probably due to relatively high level of structural disorder in the samples under investigation. The unit cell parameters of the solid-solution series PbBaFe<sub>2-x</sub>Mn<sub>x</sub>O<sub>5</sub> (0 ≤ x ≤ 1.5) are given in Table 1. With the increase of the man-

ganese content the parameters *a* and *c* increase monotonically, while the *b* parameter decreases. This result has not straightforward explanation, because the ionic radii of Fe<sup>3+</sup> and Mn<sup>3+</sup> in octahedral and five fold pyramidal coordination are almost equal – 0.645 Å and 0.58 Å, respectively [18]. One possible explanation is the Jahn-Teller effect of Mn<sup>3+</sup> atoms.

The experimental and calculated selected area electron diffraction (SAED) patterns of sample PbBaFeMnO<sub>5</sub> are given in Fig. 1. The indexing of the patterns was performed in orthorhombic lattice. The unit cell parameters were taken from powder XRD data measurements in Table 1. The reflection

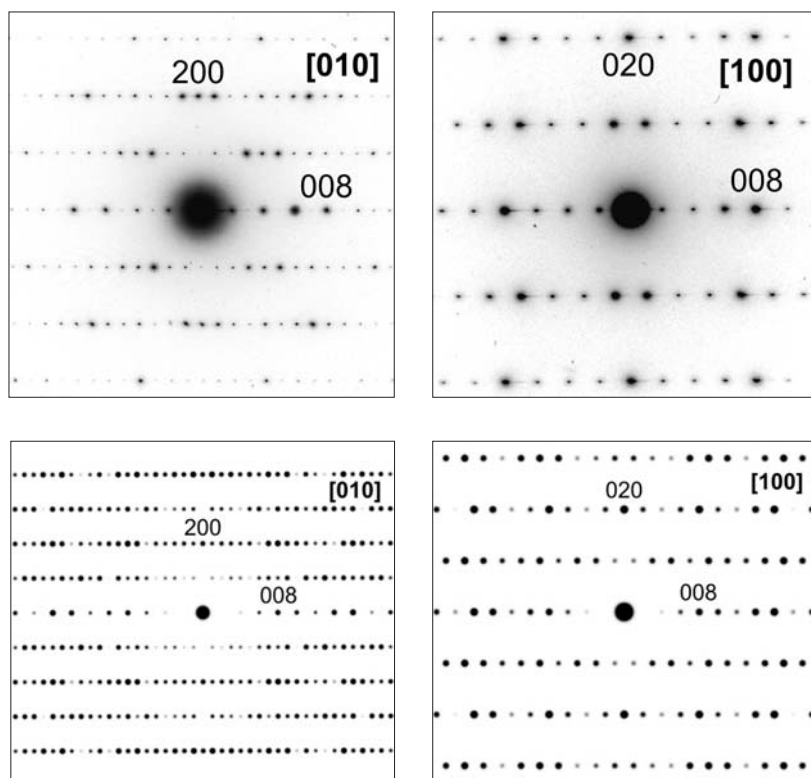


**Fig. 1.** Experimental (above) and calculated (below) SAED patterns of PbBaFeMnO<sub>5</sub> in [100] and [010] directions

conditions:  $0kl:k+l = 2n$ ,  $hk0:h = 2n$ ,  $h00:h = 2n$ ,  $0k0:k = 2n$ ,  $00l:l = 2n$  determined from the electron diffraction patterns, are in agreement with the proposed *Pnma* space group. The Rietveld refinement structural parameters of PbBaFeMnO<sub>5</sub> were used for the calculated SAED patterns in Fig. 1. The experimental data are in very good agreement with the proposed structural data.

The crystal structures of PbBaFeMnO<sub>5</sub> and PbBaFe<sub>0.5</sub>Mn<sub>1.5</sub>O<sub>5</sub> were refined using powder XRD data. The atomic positions for Pb<sub>1.08</sub>Ba<sub>0.92</sub>Fe<sub>2</sub>O<sub>5</sub> [9] were used as initial parameters for the refinement. Since the X-ray atomic scattering factors of manganese and iron are very close, their population in

the mixed occupancy positions can not be determined precisely from the Rietveld refinement data. Therefore, statistical distribution of Fe and Mn atoms in the octahedral – Fe<sub>2</sub>(Mn)O<sub>6</sub> and pyramidal – Fe<sub>1</sub>(Mn)O<sub>5</sub> sites was used.

The refined structural parameters of both samples are given in Table 2 and 3. Typical Rietveld plot of PbBaFe<sub>0.5</sub>Mn<sub>1.5</sub>O<sub>5</sub> is shown in Fig. 2. Table 4 represents calculated metal-oxygen distances and bond-valence sums in comparison with the corresponding values calculated for Pb<sub>1.2</sub>Ba<sub>0.8</sub>Fe<sub>2</sub>O<sub>5</sub> [9]. The average metal-oxygen distances around the Pb1 position inside the double chains of pyramids slightly increase with the manganese substitu-

**Table 2.** Refined structural parameters for PbBaFeMnO<sub>5</sub>  
SG: *Pnma*(62),  $a=5.7992(1)$ ,  $b=3.9099(1)$ ,  $c=21.4070(4)$ ,  $Z=4$

Atom	Wyck.	x/a	y/b	z/c	SOF	B <sub>iso</sub> (Å <sup>2</sup> )
Pb1	4c	0.0461(3)	1/4	0.5702(1)	1.00	0.72(4)
Ba1	4c	0.5594(3)	1/4	0.6854(1)	1.00	0.46(5)
Fe1	4c	0.459(1)	1/4	0.4484(2)	0.50	0.26(6)
Mn1	4c				0.50	0.26(6)
Fe2	4c	0.9328(9)	1/4	0.3152(2)	0.50	0.26(6)
Mn2	4c				0.50	0.26(6)
O1	4c	0.937(3)	3/4	0.3218(7)	1.00	1.1(2)
O2	4c	0.676(3)	1/4	0.2512(9)	1.00	1.1(2)
O3	4c	0.194(3)	1/4	0.3928(8)	1.00	1.1(2)
O4	4c	0.696(3)	1/4	0.3847(8)	1.00	1.1(2)
O5	4c	0.441(3)	3/4	0.4578(7)	1.00	1.1(2)

$R_B = 1.59$ ,  $R_{wp} = 4.95$ ,  $R_{exp} = 1.95$ ,  $GOF = 2.53$

**Table 3.** Refined structural parameters for PbBaFe<sub>0.5</sub>Mn<sub>1.5</sub>O<sub>5</sub>  
SG: *Pnma*(62),  $a = 5.8172(1)$ ,  $b = 3.8808(1)$ ,  $c = 21.5068(2)$ ,  $Z=4$

Atom	Wyck.	x/a	y/b	z/c	SOF	B <sub>iso</sub> (Å <sup>2</sup> )
Pb1	4c	0.0608(2)	1/4	0.5709(1)	1.00	0.83(3)
Ba1	4c	0.5769(3)	1/4	0.6851(1)	1.00	0.43(4)
Fe1	4c	0.4409(8)	1/4	0.4492(1)	0.25	0.28(5)
Mn1	4c				0.75	0.28(5)
Fe2	4c	0.9150(7)	1/4	0.3146(2)	0.25	0.28(5)
Mn2	4c				0.75	0.28(5)
O1	4c	0.921(2)	3/4	0.3217(5)	1.00	0.8(1)
O2	4c	0.654(2)	1/4	0.2499(6)	1.00	0.8(1)
O3	4c	0.190(2)	1/4	0.3971(6)	1.00	0.8(1)
O4	4c	0.677(2)	1/4	0.3868(6)	1.00	0.8(1)
O5	4c	0.424(3)	3/4	0.4631(5)	1.00	0.8(1)

$R_B = 1.76$ ,  $R_{wp} = 4.86$ ,  $R_{exp} = 1.90$ ,  $GOF = 2.56$

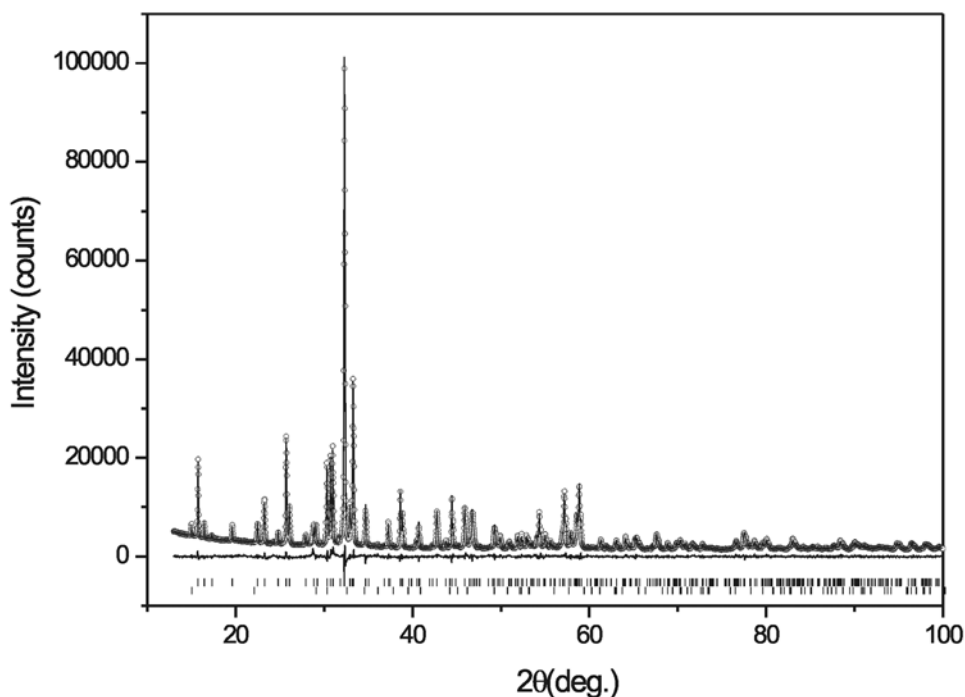


**Fig. 2.** Experimental (circles), calculated (line) and difference (bottom line) powder XRD patterns for  $\text{PbBaFe}_{0.5}\text{Mn}_{1.5}\text{O}_5$ . Lower tick bars represent peak positions for  $\text{PbBaFe}_{0.5}\text{Mn}_{1.5}\text{O}_5$  and the impurity phase  $\text{PbO}$  (Massicot)

tion. The Pb1 columns of atoms are ordered in a straight line along the  $c$  – axis in the structure of  $\text{Pb}_{1.2}\text{Ba}_{0.8}\text{Fe}_2\text{O}_5$  with coordinate  $x = 0.0032(8)$  [9]. According to the refined data for  $\text{PbBaFeMnO}_5$  and  $\text{PbBaFe}_{0.5}\text{Mn}_{1.5}\text{O}_5$ , lead atoms are considerably

shifted along the  $a$  – axis having coordinates  $x = 0.0461(3)$  and  $0.0608(2)$ , respectively (Fig. 3). The average distances in  $\text{Fe}(\text{Mn})\text{O}_5$  pyramids does not change notably. The shortest ones are observed in  $\text{PbBaFe}_{0.5}\text{Mn}_{1.5}\text{O}_5$ , mainly because of the significant

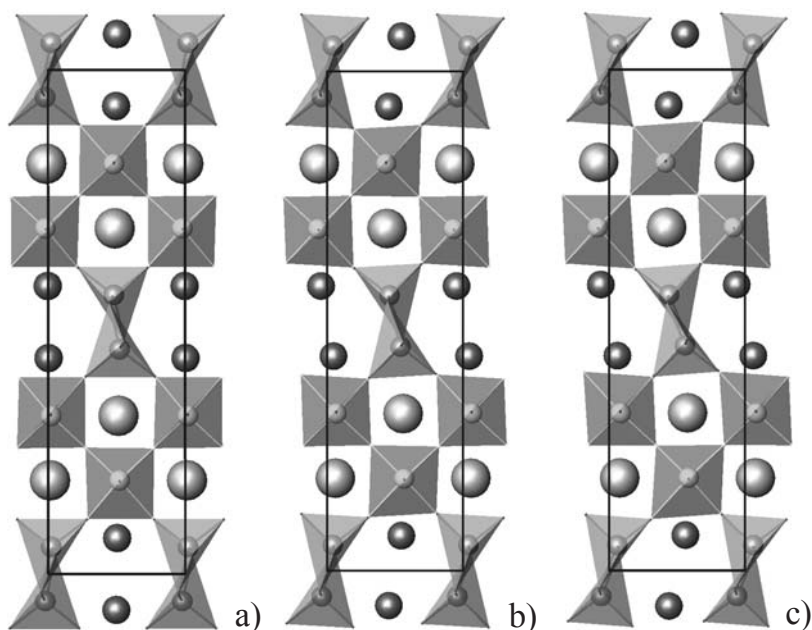


**Fig. 3.** Polyhedral representation of a)  $\text{Pb}_{1.2}\text{Ba}_{0.8}\text{Fe}_2\text{O}_5$  [9], b)  $\text{PbBaFeMnO}_5$ , and c)  $\text{PbBaFe}_{0.5}\text{Mn}_{1.5}\text{O}_5$  along  $[010]$  direction. Pyramids –  $\text{Fe}(\text{Mn})\text{O}_5$ , octahedra –  $\text{Fe}(\text{Mn})\text{O}_6$ , small dark spheres – Pb atoms, large light spheres – Ba atoms

**Table 4.** The calculated metal-oxygen distances and bond-valence sums for Pb<sub>1.2</sub>Ba<sub>0.8</sub>Fe<sub>2</sub>O<sub>5</sub>, PbBaFeMnO<sub>5</sub> and PbBaFe<sub>0.5</sub>Mn<sub>1.5</sub>O<sub>5</sub>

Metal-oxygen distances	Composition			
	Pb <sub>1.2</sub> Ba <sub>0.8</sub> Fe <sub>2</sub> O <sub>5</sub> *	PbBaFeMnO <sub>5</sub>	PbBaFe <sub>0.5</sub> Mn <sub>1.5</sub> O <sub>5</sub>	
Pb1	O(1)	2.287(9)	2.314(15)	2.312(11)
	O(3)x2	2.478(6)	2.528(11)	2.523(8)
	O(4)x2	2.631(6)	2.644(12)	2.630(8)
	O(5)	2.673(9)	2.888(17)	2.913(12)
	O(5)	3.241(9)	3.034(17)	3.085(12)
	Average	2.631(3)	2.654(5)	2.660(4)
	Valence	2.04(1)	1.88(2)	1.89(2)
Ba1	O(1)	2.873(11)	2.883(18)	2.900(12)
	O(1)	2.884(11)	2.924(18)	2.924(12)
	O(1)	2.840(12)	2.921(15)	2.939(11)
	O(2)x2	2.771(10)	2.747(13)	2.743(10)
	O(2)x2	2.836(10)	2.854(13)	2.857(10)
	O(3)x2	3.009(9)	2.943(13)	2.954(11)
	O(4)x2	2.925(9)	2.875(13)	2.887(10)
	O(5)	3.113(11)	3.064(15)	3.186(11)
	Average	2.899(3)	2.886(4)	2.903(3)
	Valence	2.36(2)	2.43(3)	2.35(2)
Fe, Mn1	O(3)	1.928(10)	1.947(18)	1.840(14)
	O(4)	1.867(10)	1.933(18)	1.921(13)
	O(5)x2	2.023(2)	1.968(2)	1.966(2)
	O(5)	2.012(8)	2.090(16)	2.043(11)
	Average	1.971(3)	1.981(4)	1.947(4)
	Valence	2.87(3)	2.77(5)	3.06(4)
Fe, Mn2	O(1)x2	1.9944(7)	1.960(1)	1.947(1)
	O(2)	1.963(12)	2.019(19)	2.059(14)
	O(2)	1.979(12)	2.006(19)	1.963(14)
	O(3)	2.106(10)	2.246(18)	2.390(14)
	O(4)	2.159(10)	2.025(18)	2.081(13)
	Average	2.033(4)	2.036(6)	2.064(5)
	Valence	2.92(3)	2.92(5)	2.82(3)

\* – The data for Pb<sub>1.2</sub>Ba<sub>0.8</sub>Fe<sub>2</sub>O<sub>5</sub> are taken from Nikolaev et al. [9].

decrease in Fe1(Mn) – O3 bond distance, which is partially compensated with the increase of Fe1(Mn) – O4 bonds. The average metal-oxygen distances in Fe2(Mn)O<sub>6</sub> octahedra monotonically increase with the substitution. The oxygen atoms O3 and O4 are common for Fe1(Mn)O<sub>5</sub> pyramids and Fe2(Mn)O<sub>6</sub> octahedra in the perovskite blocks. With increase of Mn substitution level the Fe2(Mn) – O3 bond distance increases to almost non bonding 2.390(14) Å in PbBaFe<sub>0.5</sub>Mn<sub>1.5</sub>O<sub>5</sub>. The distance Fe2(Mn) – O4 is less changed and decreases to 2.081(13) Å. The twelve-fold oxygen coordination around the Ba at-

oms does not undergo notable changes. Recently, a comprehensive study of Pb<sub>2</sub>Mn<sub>2</sub>O<sub>5</sub> employing transmission electron microscopy methods was reported [10]. This compound is synthesized under high pressure conditions as a mixture with two other phases. The proposed structural model by Hadermann et al. was found to share many common features with the Rietveld refinement results of the present samples. They report Jahn-Teller distortion of MnO<sub>6</sub> octahedra in the *a-c* plane with two long and two short Mn–O distances (see Fig. 8c, Ref. 10). The Jahn-Teller deformation of octahedral oxygen coordina-

**Table 5.**  $^{57}\text{Fe}$  Mössbauer spectral parameters of hyperfine interaction for  $\text{PbBaFe}_{1.5}\text{Mn}_{0.5}\text{O}_5$  at 300K and 77K

Site	T [K]	IS [mm/s]	QS [mm/s]	FWHM± 0.05 [mm/s]			H [kOe]	Rel area [%]
Oct(1)	300	$0.35 \pm 0.03$	$0.58 \pm 0.04$	0.21			513 ± 1	20 ± 3
Pyr(2)		$0.30 \pm 0.03$	$1.01 \pm 0.04$	0.75				19 ± 3
Oct(1)	77	$0.53 \pm 0.04$	$-0.13 \pm 0.04$	0.87	0.74	0.46	482 ± 1	48 ± 3
Pyr(2)		$0.47 \pm 0.04$	$0.1 \pm 0.04$	1.12	0.67	0.45		52 ± 3

tion around the  $\text{Mn}^{3+}$  ions is well known in many compounds and was found to be crucial for the stabilization of  $\text{Pb}_2\text{Mn}_2\text{O}_5$  structure. Similar deformation of the octahedra is observed in the crystal structure of  $\text{PbBaFeMnO}_5$  and  $\text{PbBaFe}_{0.5}\text{Mn}_{1.5}\text{O}_5$ . The degree of deformation increases with the increase of the manganese content. Most likely this is the main reason for the observed change of the unit cell parameters with the increase of manganese content (Table 1). The bond distance  $\text{Fe2(Mn)} - \text{O1}$  contracts with the increase of manganese and can be determined straight from the  $b$ -parameter. The average  $\text{Fe1(Mn)} - \text{O}$  distances also decrease with manganese substitution. Thereby, the observed increase in unit cell parameters along the  $a$ - and  $c$ -axis is mainly due to the Jahn-Teller distortion of  $\text{MnO}_6$  octahedra within the (010) plane.

The Mössbauer spectra taken at room temperature and at 77 K are presented in Fig. 4a and Fig. 4b, respectively. The parameters of the fitted spectra corresponding to an isomer shift (IS), a quadrupole splitting/shift (QS), a full width at half maximum (FWHM) of the resonance lines, a magnetic hyperfine field at the site of the Fe nucleus (H), and the relative spectral area are summarized in Table 5. The spectrum measured at room temperature was fitted by superposition of two quadrupole doublets: (1) and (2) and a continuous distribution of magnetic Zeeman sextets. The doublets (1) and (2) correspond to two iron sites in  $\text{PbBaFe}_{1.5}\text{Mn}_{0.5}\text{O}_5$  – octahedral (1) and pyramidal (2) ones, respectively. The distribution of the magnetic sextets at room temperature shows an intermediate magnetic state with the presence of a paramagnetic state (two quadrupole doublets with approximately 40% of relative spectral area), and 60% of magnetic ordering.

The Mössbauer spectrum taken at 77 K was fitted by superposition of two magnetic sextets corresponding to the two positions of magnetically ordered iron in  $\text{PbBaFe}_{1.5}\text{Mn}_{0.5}\text{O}_5$  (Fig. 4b). The broadening of magnetic components as compared to the corresponding resonance lines at 77 K for  $\text{PbBaFe}_2\text{O}_5$  [9] could be explained by random dis-

tribution of magnetic cations, Fe and Mn, at octahedral and pyramidal positions leading to different exchange interaction for the Fe–Fe and Fe–Mn cations. Actually we have two magnetic sextet distributions for the two iron sites, but for the fitting procedure an approximation was used with three different line-widths for the magnetic components of the spectra (1<sup>st</sup> – 6<sup>th</sup>), (2<sup>nd</sup> – 5<sup>th</sup>) and (3<sup>rd</sup> – 4<sup>th</sup>), as it is shown in Table 5.

Comparing with the data for  $\text{PbBaFe}_2\text{O}_5$  at 77 K [9], a diminution of the magnetic hyperfine field at the site of the Fe nucleus (H) is observed in  $\text{PbBaFe}_{1.5}\text{Mn}_{0.5}\text{O}_5$  due to the presence of manganese. Finally, our measurements show that the Mn cations replace the Fe cations for the octahedral (1) and the pyramidal (2) sites in equal proportions (within the statistical error). This result is very different from the data previously reported by us on Mössbauer spec-

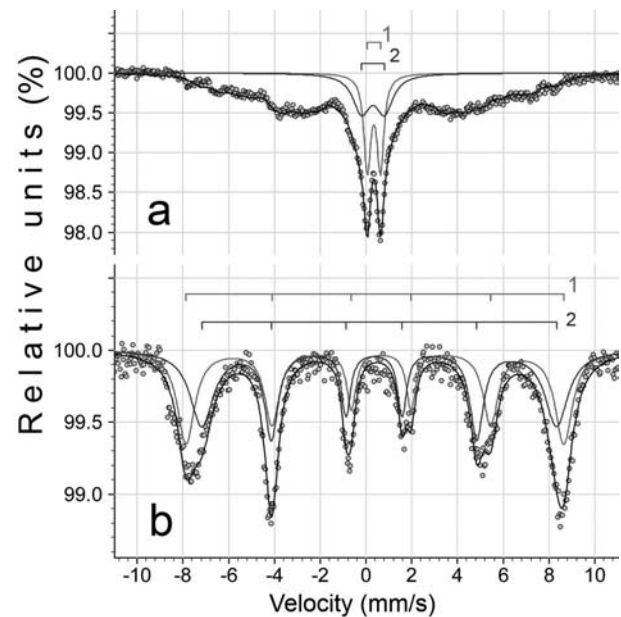


**Fig. 4.** Mössbauer spectrum of  $\text{PbBaFe}_{1.5}\text{Mn}_{0.5}\text{O}_5$  taken at a) 300K and b) 77K

troscopy of  $\text{PbBaFe}_{1.5}\text{Co}_{0.5}\text{O}_5$  [11]. The latter compound was found to have magnetic ordering at room temperature and the Co atoms were found to preferably occupy the pyramidal positions, as opposed to the new compound  $\text{PbBaFe}_{1.5}\text{Mn}_{0.5}\text{O}_5$  described in this paper.

## CONCLUSION

New solid-solution series  $\text{PbBaFe}_{2-x}\text{Mn}_x\text{O}_5$  was successfully synthesized. The members of the series are part of the homologous series  $\text{A}_n\text{B}_n\text{O}_{3n-2}$  ( $n = 4$ ). The homogeneity range was determined for  $x$  up to 1.5. The crystal structures of  $\text{PbBaFeMnO}_5$  and  $\text{PbBaFe}_{0.5}\text{Mn}_{1.5}\text{O}_5$  were refined by Rietveld method. The degree of structural deformation increases with the increase of the manganese content. This fact should be considered as the main reason for the observed changes of the unit cell parameters with the increase of manganese content. The experimental and calculated selected area electron diffraction (SAED) patterns are in very good agreement with the obtained structural data. The Mössbauer spectroscopy reveals a transition from magnetic ordering in  $\text{PbBaFe}_2\text{O}_5$  to paramagnetic state in  $\text{PbBaFe}_{1.5}\text{Mn}_{0.5}\text{O}_5$  at room temperature. The measurements at 77 K show that the Mn cations replace the Fe cations for the octahedral (1) and the pyramidal (2) sites in equal proportions.

**Acknowledgements:** We thank Ivan Spirov for his help for the Mössbauer measurements and fitting of the spectra. We thank also the National Science Fund of Bulgaria for the financial support under contract DTK-02/77 – 2009 and DO-02-224/17.12.2008.

## REFERENCES

1. M. Anderson, J. Vaughey, K. Poeppelmeier, *Chem. Mater.*, **5**, 151 (1993).
2. J. Vaughey, K. Poeppelmeier, *NIST Special Publication*, **804**, 419 (1991).
3. V. Raynova-Schwarten, W. Massa, D. Babel, *Z. Anorg. Allg. Chem.*, **623**, 1048 (1997).
4. A. Abakumov, J. Hadermann, S. Bals, I. Nikolaev, E. Antipov, G. Van Tendeloo, *Angew. Chem. Int. Ed.*, **45**, 6697 (2006).
5. J. Hadermann, A. Abakumov, I. Nikolaev, E. Antipov, G. Van Tendeloo, *Solid State Sci.*, **10**, 382 (2008).
6. D. Batuk, J. Hadermann, A. Abakumov, T. Vranken, A. Hardy, M. Van Bael, G. Van Tendeloo, *Inorg. Chem.*, **50**, 4978 (2011).
7. A. Abakumov, J. Hadermann, M. Batuk, H. D'Hondt, O. Tyablikov, M. Rozova, K. Pokholok, D. Filimonov, D. Sheptyakov, A. Tsirlin, D. Niermann, J. Hemberger, G. Van Tendeloo, E. Antipov, *Inorg. Chem.*, **49**, 9508 (2010).
8. P. Tzvetkov, N. Petrova, D. Kovacheva, *J. Alloy. Compd.*, **485**, 862 (2009).
9. I. Nikolaev, H. D'Hondt, A. Abakumov, J. Hadermann, A. Balagurov, I. Bobrikov, D. Sheptyakov, V. Pomjakushin, K. Pokholok, D. Filimonov, G. Van Tendeloo, E. Antipov, *Phys. Rev. B*, **78**, 024426 (2008).
10. J. Hadermann, A. Abakumov, T. Perkisas, H. D'Hondt, H. Tan, J. Verbeeck, V. Filonenko, E. Antipov, G. Van Tendeloo, *J. Solid State Chem.*, **183**, 2190 (2010).
11. P. Tzvetkov, D. Kovacheva, D. Nihtianova, T. Ruskov, *Z. Kristallogr. Proc. I*, 397 (2011).
12. A. Abakumov, J. Hadermann, M. Batuk, H. D'Hondt, O. Tyablikov, M. Rozova, K. Pokholok, D. Filimonov, D. Sheptyakov, A. Tsirlin, D. Niermann, J. Hemberger, G. Van Tendeloo, E. Antipov, *Inorg. Chem.*, **49**, 9508 (2010).
13. O. Korneychik, M. Batuk, A. Abakumov, J. Hadermann, M. Rozova, D. Sheptyakov, K. Pokholok, D. Filimonov, E. Antipov, *J. Solid State Chem.*, **184**, 3150 (2011).
14. TOPAS V4: General profile and structure analysis software for powder diffraction data, User's Manual, Bruker AXS, Karlsruhe, Germany Bruker AXS (2008).
15. G. Shenoy, J. Friedt, H. Maleta, S. Ruby, *Mössbauer Effect Methodology*, **9**, 277 (1974).
16. T. Cranshaw, *J. Phys. E*, **7**, 122 (1974).
17. M. Järvinen, *J. Appl. Cryst.*, **26**, 525 (1993).
18. R. D. Shannon, *Acta Cryst. A*, **32**, 751 (1976).

## СИНТЕЗ НА НОВИ $PbBaFe_{2-x}Mn_xO_5$ СЪЕДИНЕНИЯ С ПЕРОВСКИТОВ ТИП СТРУКТУРА

П. Цветков<sup>1\*</sup>, Д. Ковачева<sup>1</sup>, Д. Нихтянова<sup>1,2</sup>, Н. Величкова, Т. Русков<sup>3</sup>

<sup>1</sup> *Институт по Обща и Неорганична Химия, Българска Академия на Науките,  
1113 София, бул. „Акад. Георги Бончев“, бл. 11*

<sup>2</sup> *Институт по Минералогия и Кристалография, Българска Академия на Науките,  
1113 София, бул. „Акад. Георги Бончев“, бл. 107*

<sup>3</sup> *Институт за Ядрени изследвания и Ядрена енергия, Българска Академия на Науките,  
1784 София „Цариградско шосе“, бл. 72*

Постъпила на 22.03.2012 г.; приета на 27.04. 2012 г.

(Резюме)

Нови съединения с перовскитов тип структура и обща формула  $PbBaFe_{2-x}Mn_xO_5$  ( $0 \leq x \leq 1.5$ ) бяха синтезирани чрез твърдофазен синтез в атмосфера от аргон. Получените съединения бяха характеризирани с прахова рентгенова дифракция (XRD), ТЕМ (SAED) и  $^{57}Fe$  Мьосбауерова спектроскопия. Кристалната структура на  $PbBaFeMnO_5$  и  $PbBaFe_{0.5}Mn_{1.5}O_5$  членове на серията е определена по метода на Ритвелд. Дифракционните картини по направления  $[100]$  и  $[010]$  са получени чрез SAED. Резултатите от структурната рафинация по метода на Ритвелд са в добро съгласие с данните от електронната дифракция. Съединенията кристализират в орторомбична пространствена група  $Pnma$  и параметри на елементарната клетка  $a \approx \sqrt{2}a_p$ ,  $b \approx a_p$ , и  $c \approx 4\sqrt{2}a_p$  ( $a_p$  – параметър на перовскитовата подклетка). Кристалната структура на изучените фази се състои от перовскитови блокове отделени от  $\frac{1}{2}[110]_p(\bar{1}01)_p$  кристалографски равнини на срязване. В блоковете октаедричната В-позиция е заета от  $Fe^{3+}$  и  $Mn^{3+}$  йони и дванадесет координираната А-позиция е изцяло заета от  $Ba^{2+}$  йони. Перовскитовите блокове са свързани помежду си с двойни вериги от изкривени  $(Fe, Mn)O_5$  тетрагонални пирамиди, които споделят общи ръбове. Веригите са по протежение на  $b$ -оста и ограничават шестоъгълни тунели запълнени изцяло от  $Pb^{2+}$  катиони. Пирамидалните вериги имат две огледално свързани конфигурации („лява“ – L и „дясна“ – R), като слоеве изградени само от една от двете конфигурации се редуват по протежение на  $c$ -оста в  $-L-R-L-R-$  последователност. Мьосбауеровата спектроскопия на  $PbBaFe_{1.5}Mn_{0.5}O_5$  показва, че с увеличаване на заместването на  $Fe^{3+}$  от  $Mn^{3+}$  катиони температурата на прехода от магнитно подредено в парамагнитно състояние се понижава. Направените измервания при 77 К показват, че  $Mn^{3+}$  замества  $Fe^{3+}$  в октаедричната и пирамидална позиции в еднаква степен.